

ASSESSMENT OF POTENTIAL SUITABILITY OF LAND FOR TOWN GROWTH – FRANZ JOSEF**COMPARATIVE HAZARD ASSESSMENT OF EXISTING AND PROPOSED FRANZ JOSEF TOWN SITES:
PROGRESS REPORT FOR WESTLAND DISTRICT COUNCIL****APRIL 2022**

Tim Davies

School of Earth and Environment, University of Canterbury

1. Introduction

On 20 Dec 2020 WDC contracted UC to provide a comparative hazard assessment of the existing and proposed Franz Josef town sites (Fig. 1, 2). This work is to be carried out by Dr Tim Davies and a MSc thesis student, Nandhini R.

Reported data are to include

- the approximate footprints of the identified hazards over a range of magnitudes and frequencies on both present and proposed town sites;
- a comparison of the average annual hazard impact on the present town site with that of the proposed new site, assuming the same degree of development at each site;
- identification of specific areas requiring more detailed investigation.

The present progress report deals with the first of these.

The MSc thesis, which will be submitted at the end of May 2022, will provide a full account of the project and a comprehensive quantitative comparison of the hazard exposure of the sites. The work is at the stage where all the required hazard information has been assembled, and this report provides a summary of the degree to which the two sites are potentially affected by the hazards. The hazards considered are river flooding, earthquake, landslide, liquefaction, dambreak flooding, and debris flow.

The thesis content will be summarised in a Final report.

2. Background

Future hazards at Franz Josef are expected to alter with time due to (i) climate change and (ii) earthquake occurrence. Climate change has been ignored in the present work because, first, it is a relatively slow process whose impacts will take many years to become fully apparent and in the meantime it is sufficiently accurate to predict future climate-related hazards based on past experience of these; and, second, climate change impacts, while still seriously debated, are likely to be similar for both present and proposed town sites and so will not significantly affect the relative hazard vulnerability of the sites.

Earthquake occurrence at Franz Josef is dominated by the expectation of a major earthquake on the Alpine fault or on a different fault in the Southern Alps. This probability of this event is about 75% in the next 50 years, according to research by Victoria University (Howarth et al., 2021). Following this earthquake, the hazard probabilities at Franz Josef over the following decades to century will change significantly, because of the large volume of earthquake-generated landslide sediment that will be deposited in rivers and the severe aggradation and increased flooding this will cause (Blagen et al., in

review). It is not presently feasible to anticipate quantitatively how the hazardscape will be affected by the next major earthquake.

Because of this, the present work considers only the current, pre-earthquake hazard distribution (which however includes the immediate impacts of the earthquake itself) in comparing the hazard exposures of the two town sites.

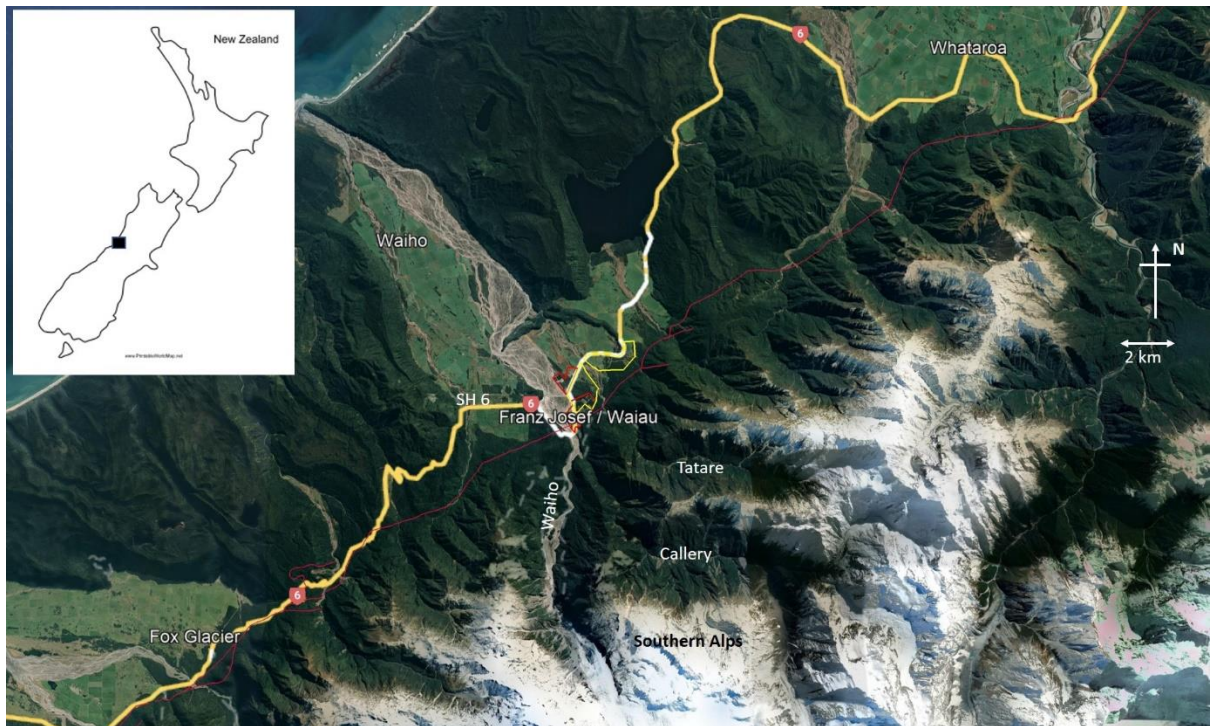


Fig. 1 Franz Josef area, Westland showing location relative to Alpine fault (red line), SH 6 (yellow line), Southern Alps and major rivers. Modified Google Earth image.

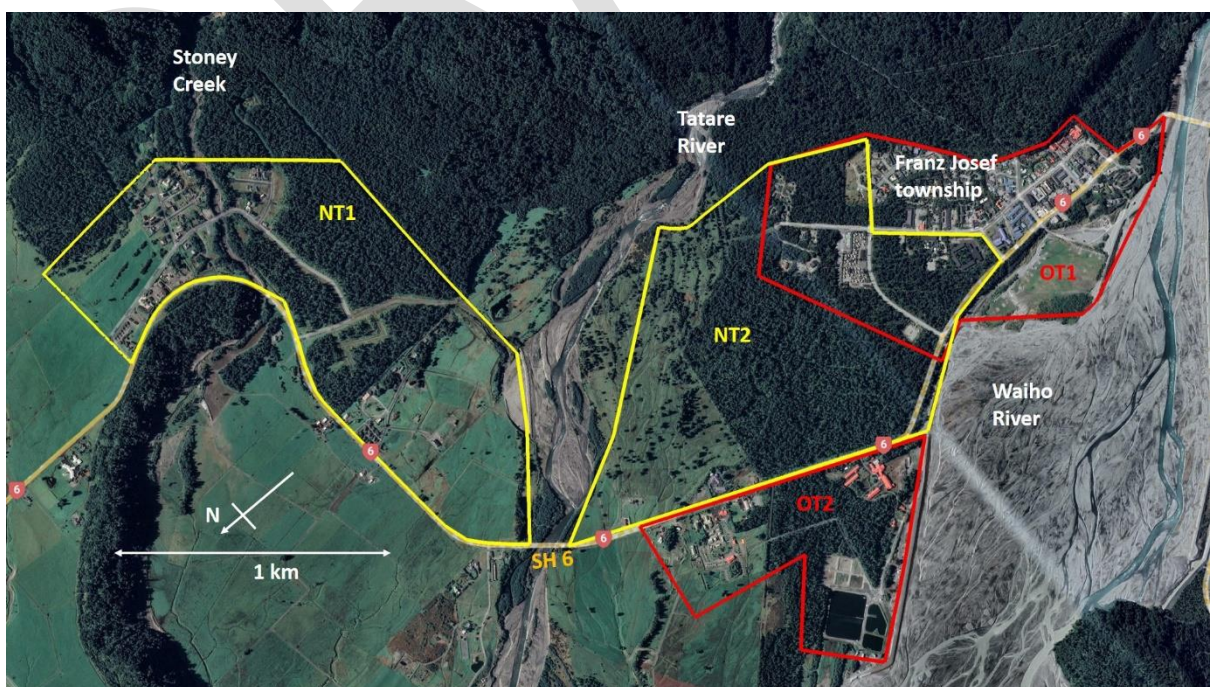


Fig. 2 Close-up of Franz Josef township area showing present town sites (red lines: OT1 and OT2) and proposed town sites (yellow lines: NT1 and NT2)

3. Assumptions

We assume that:

- 3.1 The spatial distribution of assets within the two town sites is uniform. Thus the impact of each hazard event is characterised only by the spatial distribution of the hazard event itself, not by the location of any specific asset. The hazard spatial distribution, however, provides information that may be useful in deciding where to locate assets across the two sites in order to reduce impacts. Similarly, risk-to-life estimates will be based on assumed uniform distributions of people across the two sites at a range of densities starting from pre-Covid permanent and tourist populations.
- 3.2 Stopbanks are present as planned in 2020, including raising of existing banks and installation of a bank to prevent the Waiho avulsing into the Tatare downstream of the oxidation ponds (Figs 3, 4). We assume also that these stopbanks operate as designed.
- 3.3 The Waiho River continues aggrading. Beagley et al. (2020) showed that if the Waiho behaves over the next century as it has during the last 50 years (aggrading at about 0.17 m/year), its bed will aggrade by about 17 m at the SH6 bridge by 2120, assuming that it remains confined in its present bed by raising stopbanks. To manage this situation, the West Coast Regional Council medium-term strategy is to relax/remove the western stopbanks (true left of the Waiho River) so that the flood threat to the east bank (true right) land is greatly reduced (Gardner, 2021). Thus the eastern stopbanks only need to function until this is achieved; they have been designed to cope with about 20 years of aggradation (Gardner, 2021), so this is the corresponding time-scale over which the present work applies. Note also that the probability of a major earthquake in the next 20 years is about 30%; this event will drastically alter (increase) the subsequent flood risk due to large coseismic landslide sediment input to the river (Robinson et al., 2016; Briggs et al., 2018).

4. Hazards and data

Outlined herein are the data sources, and estimated spatial extents and recurrence intervals, for known hazards of the area: river flooding, earthquake (surface rupture, ground shaking and liquefaction), earthquake-triggered rock avalanche, landslide dambreak flooding and debris-flow events. The quantities used in these estimations are necessarily approximations, because few data exist describing the magnitude-frequency relationships of these events. Hence the areas delineated as affected by events of specific return periods, though as realistic as possible, are also approximations. Even if these delineations were ideally accurate, however, they would not in any case predict the affected areas of any specific future events. Nevertheless, as statistical approximations they are useful for comparing the hazard exposures and risk levels in the township areas.

The areas affected by events of different return periods are in some cases the result of state-of-the-art numerical simulations (Waiho River flooding and landslide dambreak flooding), while others (rock avalanche, debris flow, earthquake) are based on empirical data from within New Zealand and from overseas.

The ranges of return periods vary between hazards. Thus, for example, we delineate the area affected by a 100,000-year return period rock avalanche because, although it has a very low probability (10^{-5}) of occurring in any given year, it poses a high risk to life because it can kill a large number of people. The occurrence of earthquakes, however, is dominated by the Alpine fault

earthquake which currently is a 50 – 100-year return interval event and is also the maximum conceivable event for the area; earthquakes and landslides have very different magnitude-frequency distributions.

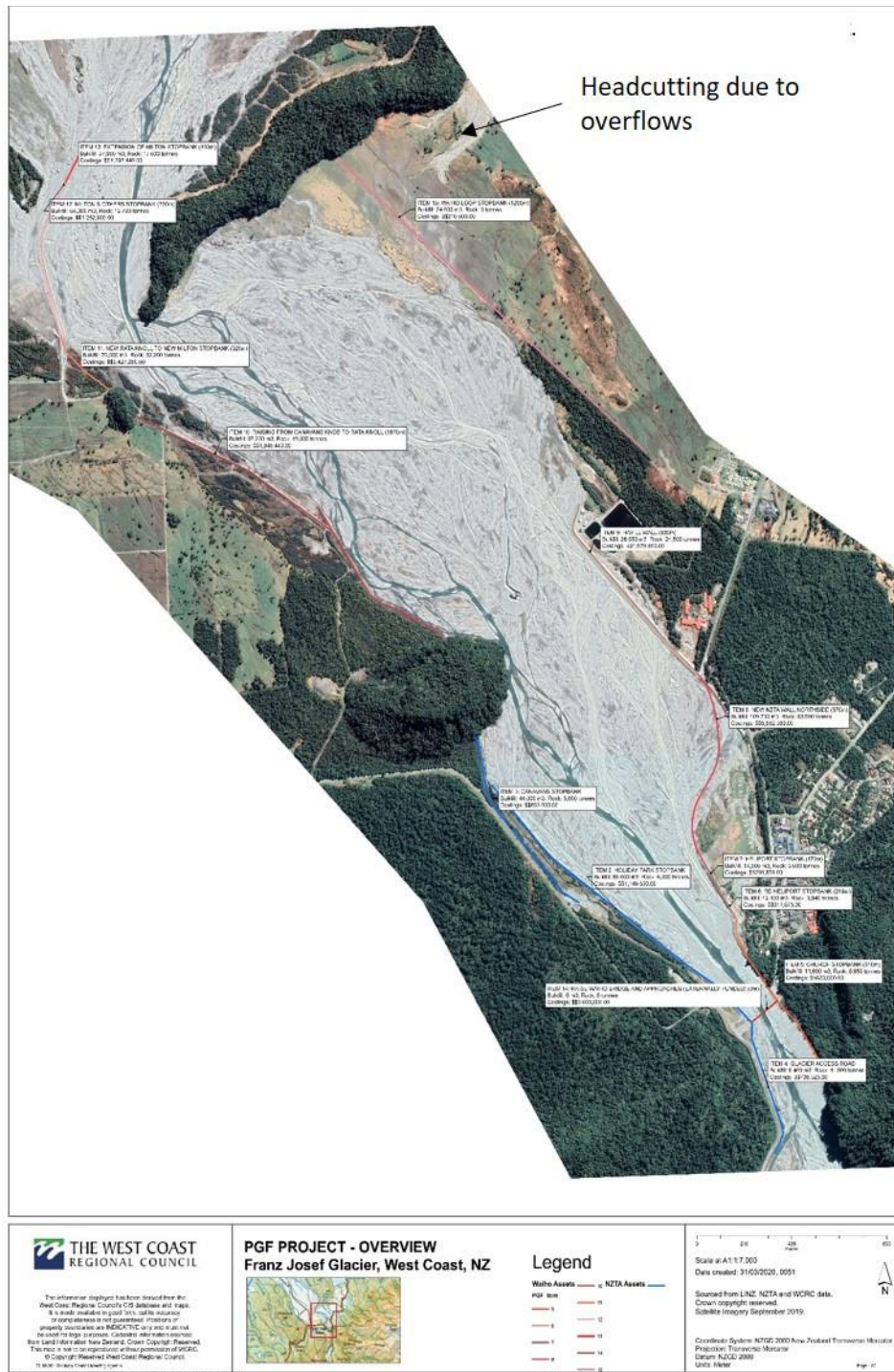


Fig. 3 Planned stopbanks (red) at Franz Josef

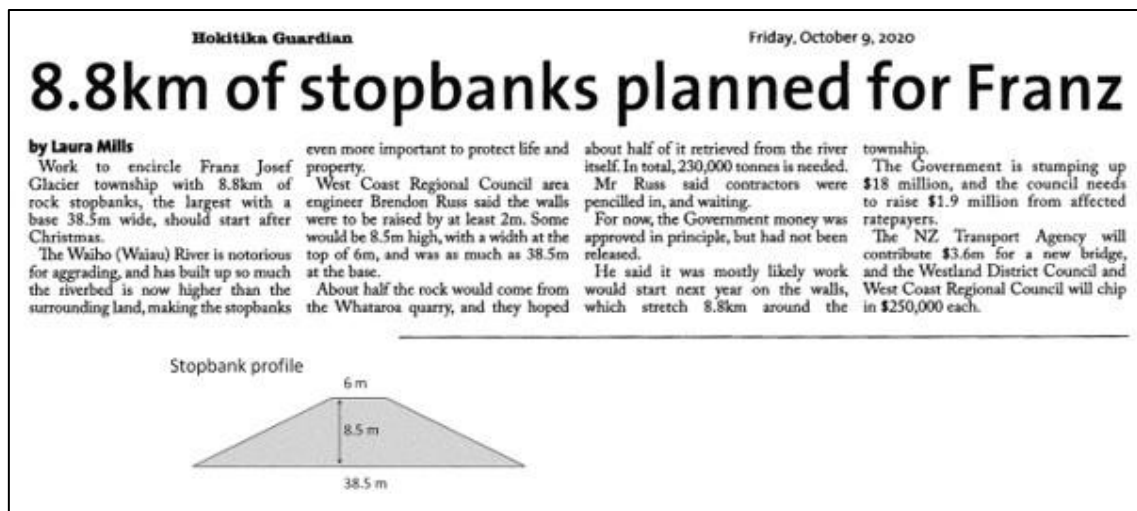


Fig. 4 Information and cross-section of planned stopbanks

4.1 River flooding:

(a) Waiho River

The area of land threatened by flooding from the Waiho River has been modelled by Gardner (2021), based on the stopbanks planned in 2020, but omitting consideration of the new bank planned to extend from the vicinity of the oxidation ponds to the Waiho Loop; this is designed not to overtop at flows below $2500 \text{ m}^3\text{s}^{-1}$. These stopbanks are designed on the basis of current bed levels plus 20 years' aggradation at about 0.18 m/year (Gardner, 2021). The flooded areas have been modelled for discharges of 500 to $3500 \text{ m}^3\text{s}^{-1}$, and Fig. 5 indicates the flooding extent for $2500 \text{ m}^3\text{s}^{-1}$, about a 100-year flood; it is notable that there is no threat to either town site as long as the stopbanks remain functional.

Table 1 Flood magnitude and frequency, Waiho River (derived from Gardner, 2014)

Return period, years	Discharge, m^3s^{-1}
20	1857
50	2128
100	2330
400	2735
500	2800
1000	3000
5000	3300
10000	3500

(b) Tatara River

Flooding of the Tatara River has not been an issue previously because the river bed is incised below the general land surface from the SH6 bridge downstream, with the depth of incision increasing to over 10 m at the Waiho Loop. However parts of the western new town site (NT2) adjacent to the Tatara upstream of the SH6 bridge are likely to be prone to flooding in severe rainstorms, especially if there are substantial sediment inputs in the Tatara catchment. The return period of this extent of inundation is arbitrarily assigned as 100 years,

As pointed out by Davies et al. (2013), overflows from the Waiho into the Tatare immediately upstream of the Waiho Loop are occurring increasingly during high flows, and the ca 10 m lower elevation of the Tatare bed causes headward erosion that tends to increase these flows (indicated in Fig. 2). If a substantial proportion of Waiho floods in due course enters the Tatare then aggradation of the Tatare is to be expected, which can then progressively increase the bed level upstream. Modelling by Davies et al. (2013) indicated that flooding of the Tatare upstream of the SH6 bridge may be exacerbated due to this aggradation. It is to prevent this that the planned stopbank upgrades include a bank extending from the oxidation ponds to the Waiho Loop designed to contain Waiho flows of $2500 \text{ m}^3\text{s}^{-1}$ (Gardner, 2021) which is about a 200-year event (Table 1). We assume that this bank will prevent such overflows as designed.

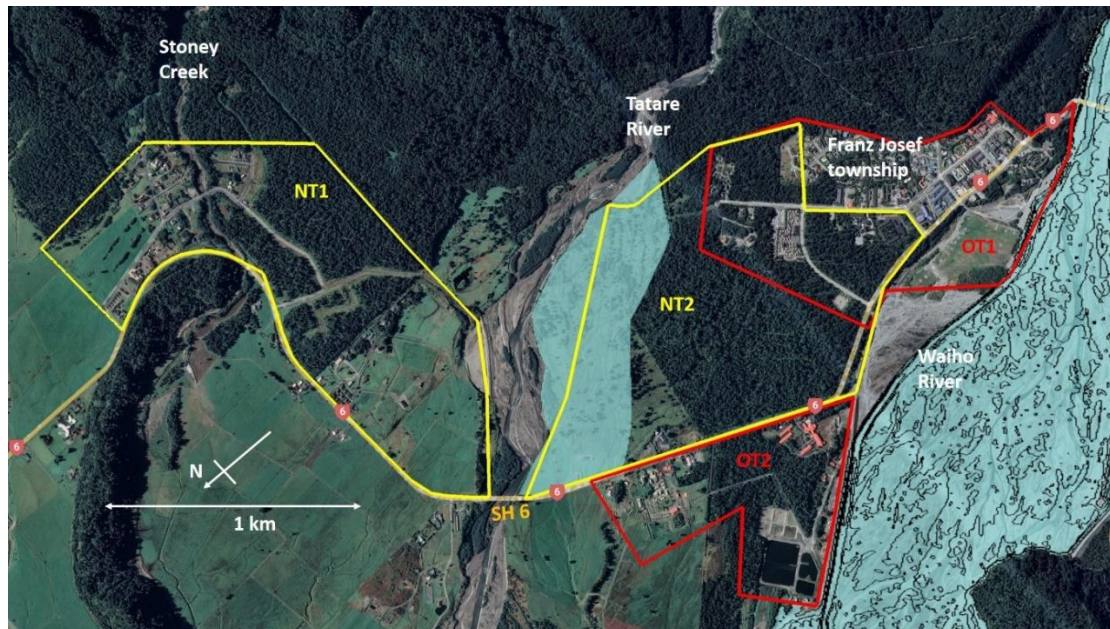


Fig. 5 Flood hazards at Franz Josef from Tatare and Waiho Rivers, ca 100-year return interval

Note that with the planned stopbanks in place, no flooding of any of the town sites from the Waiho is anticipated over the next 20 years. After that, ongoing river aggradation will increase the probability of stopbank failures; it is not feasible to generally model that situation because the flooding location, intensity and extent will depend on the location and nature of the failure which are not predictable.

4.2. Earthquake: Alpine fault

The Alpine fault delineates the western rangefront of the Southern Alps, and is known to have ruptured several times per millennium with earthquakes of M_w 8 or greater; Howarth et al. (2021) estimated that the next such earthquake has a 75% probability of occurring in the next 50 years, with a current annual probability of 1-2% (50 to 100-year return period).

The surface trace of the last (1717) rupture of the Alpine fault passes through the present township site and is delineated by the Fault Rupture Avoidance Zone (FRAZ; brown area in Fig. 6) that was designated by WDC in 2010 but rescinded in 2016. In this zone ground rupture is anticipated during the earthquake, with consequent destruction of assets and corresponding risk to life. This affects only the present town site OT1 (Fig. 6).

The other major consequence of the earthquake is ground shaking; this is shown by Langridge et al. (2016) to be essentially uniform across all of the town sites, with a peak ground acceleration

of greater than $0.75g$ (7.5 ms^{-2} , corresponding to Modified Mercalli Scale X – XII, which means severe damage to buildings); this aspect of earthquake hazard is thus identical across both present and future sites.

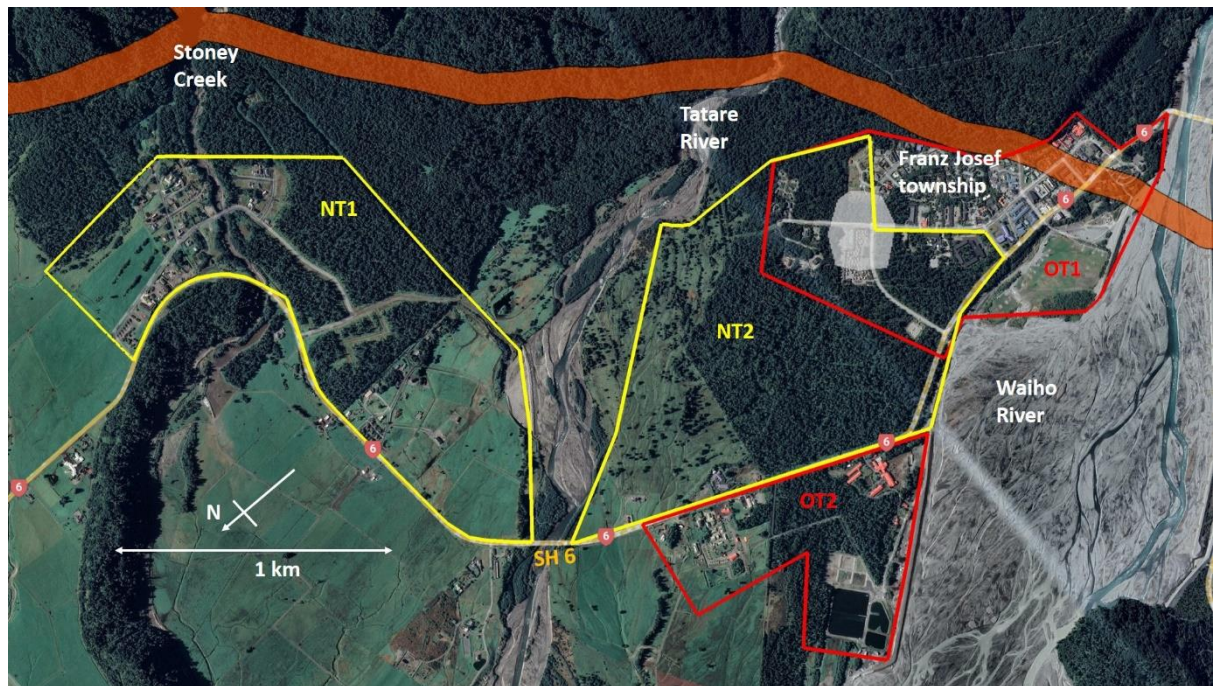


Fig. 6 Earthquake-related hazard at Franz Josef. Brown = surface rupture zone. Note whole area shown is affected by shaking $> 0.75g$; white area = risk of liquefaction. Return periods ca 50-100 years.

4.3 Liquefaction

Earthquake shaking will also cause liquefaction to occur at one location (Fig. 6) identified by Langridge et al. (2016). This location is within both the present and the proposed town sites, so again its impact is identical to both. Given the relatively coarse gravels that make up the alluvial sediments in the area, however, liquefaction seems unlikely to contribute significant additional shaking-derived damage in Franz Josef. If liquefaction accompanies Alpine fault earthquakes, as seems likely, then the return period is the same as that of ground rupture, or about 50-100 years

4.4 Earthquake-triggered landslide

Langridge et al. (2016) describe a potential major landslide (rock avalanche) that could fall from the hillslope overlooking Franz Josef during an earthquake on the Alpine fault that crosses the foot of the slope. Davies and Moretti (2021) estimated a potential failure volume of the order of 10^7 m^3 for this event, and an annual probability of the order of 10^{-5} , or 1 in 100,000. We have derived a relationship between landslide volume and probability from New Zealand data (Korup and Clague, 2009), and the corresponding deposit extents (Table 2) from an empirical volume-runout relationship (Davies, 1982); these are shown in Fig. 7. Note, however, that the smallest event listed has a return period (60 years) far shorter than that of the trigger event (Alpine fault earthquake), so this is probably a statistical fiction. Similarly, a 10^8 m^3 rock avalanche would affect all but the northern half of NT2, but the ability of the source slope to yield such an event is extremely doubtful, and it would have a return period of about 4 million years, so is not considered a realistic hazard.

It is worth noting that Davies and Moretti (2021) estimated the risk-to-life presented to the present town site OT1 by the 10^7 m^3 event (with an assumed 100,000-year return interval) to be about 10^{-2} per year, which is about 100-1000 times higher than internationally-used levels of acceptable risk. If the 10^6 m^3 event with a 2500-year return interval is a realistic possibility then the risk-to-life is about 40 times higher still, because even this smaller event can overwhelm the township.

Table 2 Rock avalanche volume, runout distance and return period

Volume, m^3	Probability, a^{-1} *	Runout, km^{**}	Return period (yr)
10^{5***}	1.6×10^{-2}	0.5	60
10^6	4×10^{-4}	1.0	2,500
10^7	1×10^{-5}	2.1	100,000

*Korup and Clague (2009) based on $p(10^7 \text{ m}^3) = 10^{-5} \text{ a}^{-1}$. **Davies, 1982. *** statistical fiction

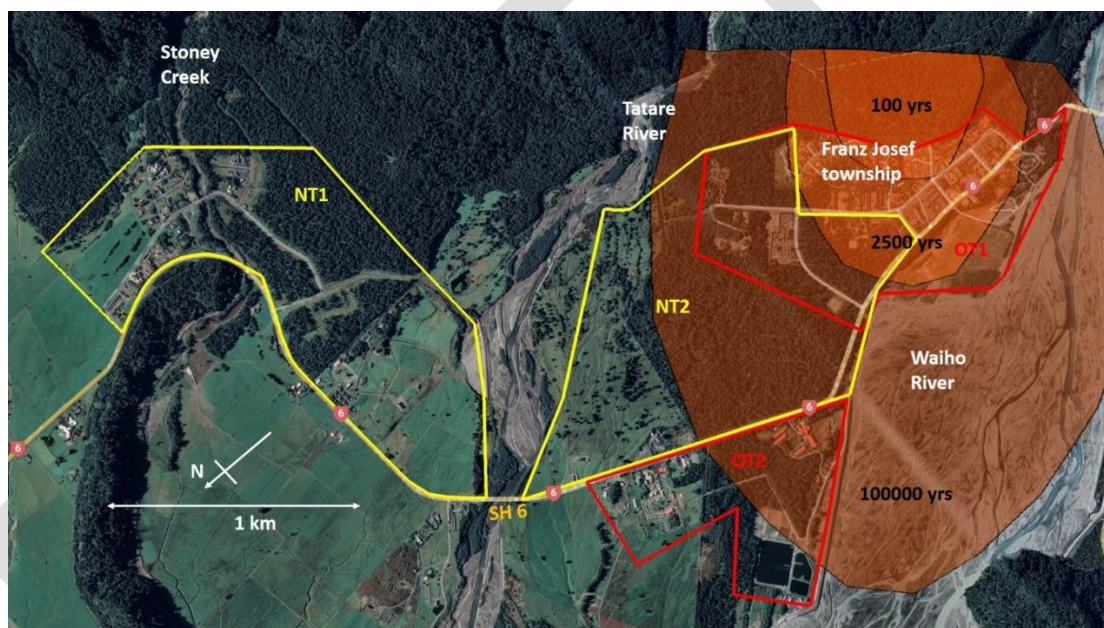


Fig. 7 Landslide (rock avalanche) hazard at Franz Josef

4.5 Landslide dambreak flooding

Landslides in the mountains east of the Alpine fault take place in steep terrain through which run deeply-incised rivers. A major landslide in this terrain has a high probability of blocking a river by forming a temporary “landslide dam”. The lake formed behind this will in due course overtop the dam and can cause it to fail, either immediately or some time later; the release of the impounded lake water then causes a flood to move through the downstream river system, often carrying large quantities of woody debris and sediment. Such an event in the Poerua River in 1999 took place a week after the landslide occurred and caused significant damage to farmland downstream. Note that this landslide was neither earthquake- nor rainfall-triggered. Dambreak flood peaks are usually very high compared to those of normal floods, and correspondingly affect larger areas; they are also more difficult to forecast for warning and evacuation purposes. An event of this type affecting Franz Josef township would cause severe damage and threaten lives.

Franz Josef is vulnerable to landslide dambreak floods in the Callery and Tatare Rivers, both of which flow between steep, high slopes for much of their lengths. The Callery is a major tributary of the Waiho with its confluence about 1 km upstream of the township (Fig. 1). Ollett (2001), Davies (2002) and Dunant et al. (2021) quantified the hazard due to landslide dambreak flooding in the Callery River (Table 3), as a result of which the Franz Josef Holiday Park was relocated from its riverside site in 2003. R (2021) similarly quantified the hazard from the Tatare River (Table 4), which had not been investigated previously. GNS Science, through its Endeavour research programme (Massey, C.I., GNS Science Ltd, PO Box 30368 Lower Hutt, *pers. comm.* 2022), used a RAMMS model to simulate dambreak flood flows of a range of return intervals from both catchments, together with the areas these events would impact (Figs 8 - 10). Note that these dambreak discharges from the Callery and Tatare Rivers assume only minor background flows.

Table 3 Callery-Waiho landslide dambreak flood magnitude-frequency (from Dunant et al., 2021).

Peak discharge m^3s^{-1}	1000	2000	3000	4000	5000	6000	7000	8000	9000
Return period years	5	15	25	45	75	100	175	300	2000

Table 4 Tatare landslide dambreak flood magnitude-frequency (R, 2021)

Peak discharge m^3s^{-1}	1000	2000	3000	4000	5000	6000	7000	8000	9000
Return period years	40	75	100	330	500	700	950	2100	4000

These simulations used the unmodified 2016 DEM for the area, and thus the 2016 stopbank levels. Therefore the areas shown flooded by the 50- and 100-year return period dambreak flows (Figs 8 & 9) are not constrained by the planned stopbanks (Fig. 3). This is because a landslide dambreak flood differs considerably from a normal rainstorm flood, in particular by assuming some of the characteristics of a debris flow surge with a deep, tree-and-boulder laden main surge that may overtop stopbanks designed to contain normal floods. The simulations accounted for the higher mean sediment concentration of a dambreak flood, but not for its rapidly-varied flow. The highest return period events (Fig. 10) would in any case overtop the planned stopbanks.

Note that Davies and Korup (2007) found evidence of intense sedimentation close to the liquefaction site (Fig. 6) which they interpreted as caused by a prehistoric dambreak flood from the Tatare.

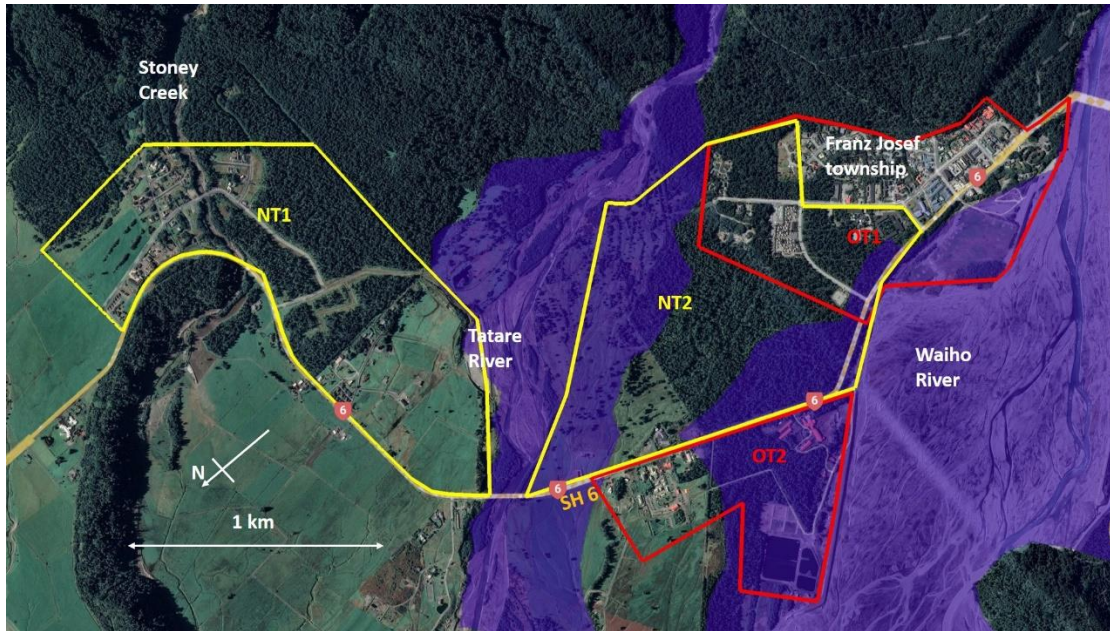


Fig. 8 Extent of ca 50-year return interval landslide dambreak flooding from the Callery (right, $4200 \text{ m}^3\text{s}^{-1}$) and Tatare ($1000 \text{ m}^3\text{s}^{-1}$) Rivers

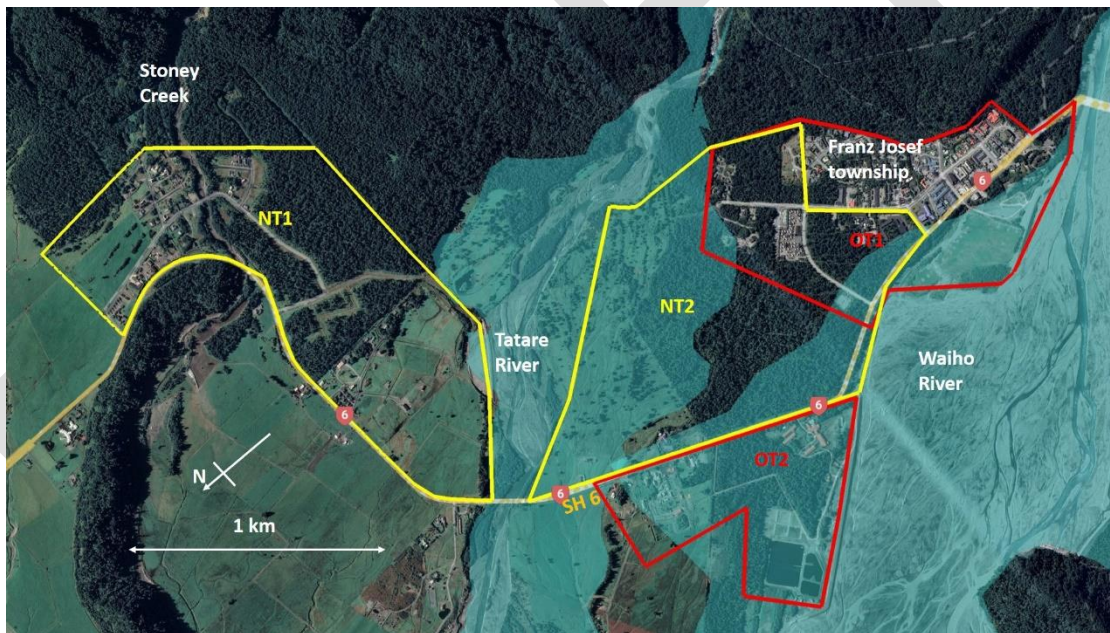
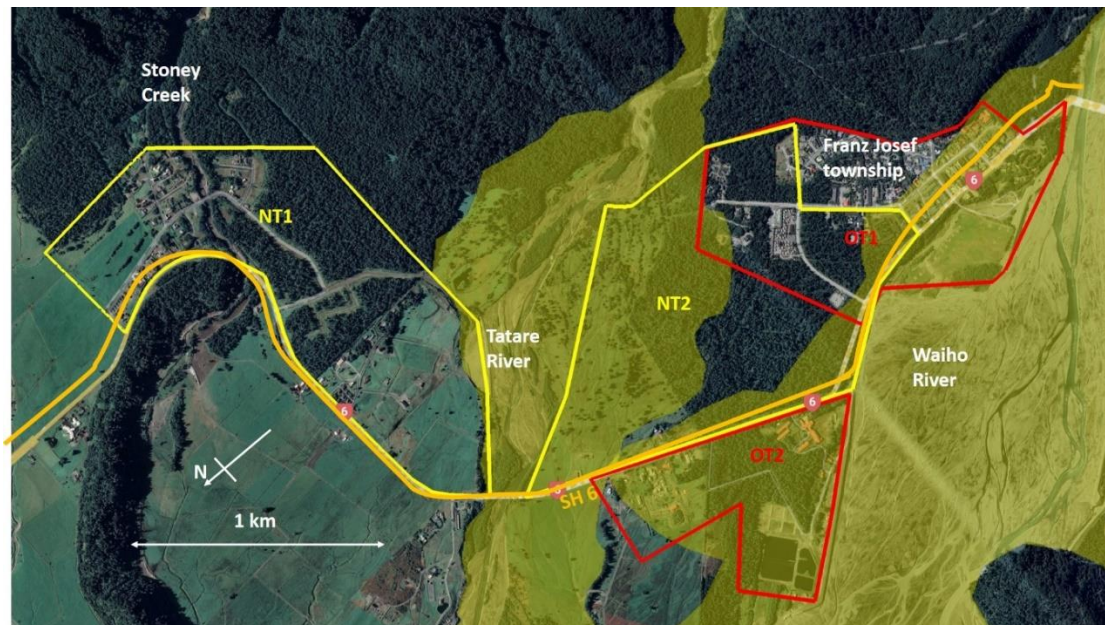


Fig. 9 Extent of ca 100-year return interval landslide dambreak flooding from the Callery-Waiho (right, $6000 \text{ m}^3\text{s}^{-1}$) and Tatare ($2500 \text{ m}^3\text{s}^{-1}$) Rivers



. Fig. 10 Extent of ca 300-year return interval landslide dambreak flooding from the Callery-Waiho (right, $8000 \text{ m}^3\text{s}^{-1}$) and ca 500-year return period flooding from the Tatare ($5000 \text{ m}^3\text{s}^{-1}$)

4.6 Debris flows

Debris flows are severe sediment-flood events that occur occasionally in small, steep catchments, and are capable of causing devastating damage to assets as demonstrated by the 2005 event at Matatā, Bay of Plenty; they also pose a serious threat to life. The catchment of Stoney Creek has been identified as prone to debris flows (Welsh and Davies, 2011), but there are no data available to quantify the magnitude-frequency relationship of this phenomenon at this site. We therefore adopted published international empirical relationships based on catchment area to assess the likely magnitudes and deposit areas of debris flows from Stoney Creek. We also assumed that such flows would result from rainfall-induced landslides in the Stoney Creek catchment, and that these would follow the magnitude-frequency relationship established for such events in the western Southern Alps by Hovius et al. (1997); see Table 5. It is noted that this ignores the potential for debris flows to mobilise streambed sediments in the catchment and on the fan, so our estimates of volume are likely on the low side; however the catchment is short and very steep so this error is unlikely to be large. The areas affected by these flows are shown in Fig. 11.

Note that this is the pre-earthquake hazard, since the Hovius et al. (1997) data refer to non-seismic conditions. Following a major earthquake there is likely to be a large volume of available coseismic landslide sediment in the catchment, so the occurrence of a debris flow in subsequent intense rainstorms has a very high probability.

Table 5 Stoney Creek debris-flow magnitude-frequency

Debris flow volume m ³	Return period years
1000	500*
5000	100
10000	100
20000	150
50000	500
100000	1000
200000	2500

* Rollover at low volume causes higher return period; see Hovius et al. (1997).

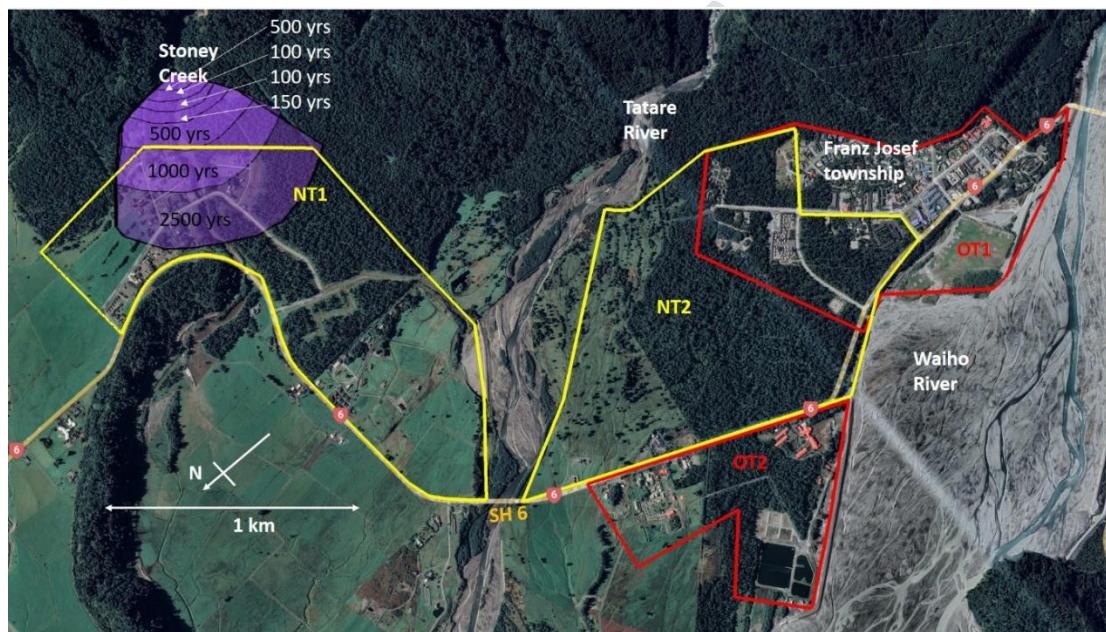


Fig. 11 Debris-flow hazards at Franz Josef

5. All hazards

Combining all the above hazards shows all the hazards affecting the present and proposed town sites (Fig. 12). Note these are for various return periods; debris flows (blue) 500, 1000 and 2500 years, rock avalanche (brown) 100, 2500 and 100,000 years, landslide-dambreak flood (yellow) 300 years (Callery) and 500 years (Tatare), ground rupture (brown) and liquefaction (white), 50-100 years; and river flooding (light grey), 100 years. While the mix of return periods precludes detailed conclusions, some trends are clear:

- Much of the current township (OT1 and OT2) and most of the present Stoney Creek development are hazard-affected
- About 80% of NT1 and 30% of NT2 are free of known hazards except for ground shaking

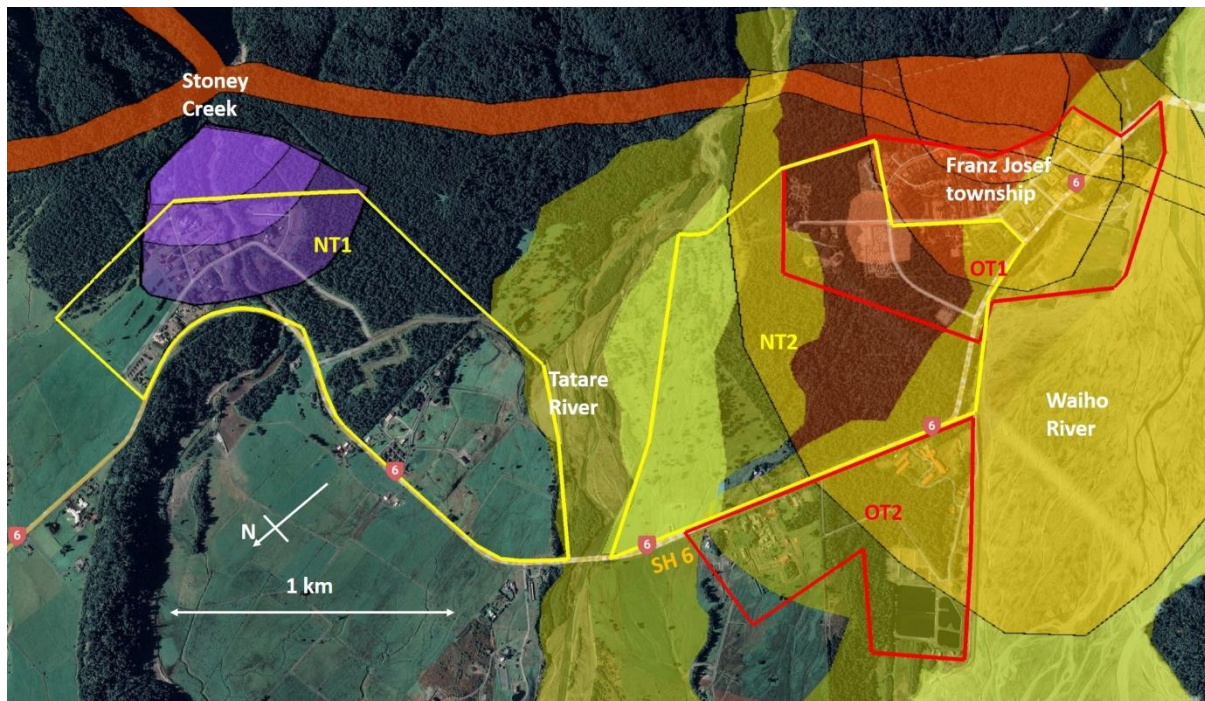


Fig. 12 All hazards affecting present and proposed town sites

6. Comments

While the information in this progress report gives a general view of hazard extents and return periods, it is not easily quantified for numerical comparisons. Hence the MSc thesis of Nandhini R and the final project report will supplement the present return period maps with GIS-based annual probability distributions, which can be summed to give the total hazard occurrence probability for each town site area. Assuming uniform spatial distribution of assets and people, and equal degrees of threat from each hazard, these hazard occurrences can be replotted as risk-to-asset and risk-to-life distributions.

There are some empirical data available that describe the relative threats to life posed by various types and intensities of hazard (e.g. probability of death related to local flood depth and to landslide inundation depth). An attempt will be made to refine the life-risk distributions of the various sites on this basis.

These spatial distributions will contribute to decision-making regarding the potential relocation possibilities for Franz Josef, and will provide indications as to where are the best locations for specific infrastructures such as medical centres, schools and aged facilities, in order to minimise total risks to assets and lives.

7. Acknowledgements

Matthew Gardner of Land, River, Sea Consulting Ltd kindly provided flooding data for the Waiho River. Chris Massey of GNS Science Ltd carried out simulations and made available data for landslide dambreak flooding from the Waiho and Tatare rivers. Tom Robinson of University of Canterbury provided constructive comments throughout.

8. References

- Beagley, R.P.J., Davies, T.R.H. and Eaton, B., 2020. Past, present and future behaviour of the Waiho River, Westland, New Zealand: A new perspective. *Journal of Hydrology (New Zealand)*, 59(1), pp.41-61.
- Blagen J.R., Davies T.R.H., Wells A., Norton D.A. (in review) Post-seismic aggradation history of the West Coast, South Island, Aotearoa/New Zealand; dendrogeomorphological evidence and disaster recovery implications. *Natural Hazards*.
- Briggs, J., Robinson, T.R. and Davies, T.R.H., 2018. Investigating the source of the c. AD 1620 West Coast earthquake: implications for seismic hazards. *New Zealand Journal of Geology and Geophysics*, 61(3), pp.376-388.
- Davies, T.R.H. (1982) Spreading of rock avalanche debris by mechanical fluidization. *Rock Mechanics* 15 (1):9-24.
- Davies, T.R.H., 2002. Landslide-dambreak floods at Franz Josef Glacier township, Westland, New Zealand: a risk assessment. *Journal of Hydrology (New Zealand)*, pp.1-17.
- Davies, T.R.H. and Moretti, D., 2022. Geomorphic precursors of large landslides: seismic preconditioning and slope-top benches. In Davies, T.R.H. and Rosser, N.J. (Eds) *Landslide Hazards, Risks, and Disasters* 2nd Edition. Elsevier, pp. 641-666.
- Davies, T.R.H., Campbell, B., Hall, B. and Gomez, C., 2013. Recent behaviour and sustainable future management of the Waiho River, Westland, New Zealand. *Journal of Hydrology (New Zealand)*, pp.41-56.
- Dunant, A., Bebbington, M., Davies, T.R.H. and Horton, P., 2021. Multihazards Scenario Generator: A Network-Based Simulation of Natural Disasters. *Risk analysis*, 41(11), pp.2154-2176.
- Gardner, M., 2021. Franz Josef stopbanks – preliminary design report. *Report to West Coast Regional Council*, 26 October 2021, 27p + app.
- Hovius, N., Stark, C.P. and Allen, P.A., 1997. Sediment flux from a mountain belt derived by landslide mapping. *Geology*, 25(3), pp.231-234.
- Howarth, J.D., Barth, N.C., Fitzsimons, S.J., Richards-Dinger, K., Clark, K.J., Biasi, G.P., Cochran, U.A., Langridge, R.M., Berryman, K.R. and Sutherland, R., 2021. Spatiotemporal clustering of great earthquakes on a transform fault controlled by geometry. *Nature Geoscience*, 14(5), pp.314-320.
- Korup, O. and Clague, J.J., 2009. Natural hazards, extreme events, and mountain topography. *Quaternary Science Reviews*, 28(11-12), pp.977-990.
- Langridge, R.M., Howarth, J.D., Buxton, R. and Ries, W.F., 2016. Natural hazard assessment for the township of Franz Josef, Westland District. *GNS Science consultancy report 2016*, 33, p.61.
- Ollett, P.P., 2001. Landslide dambreak flooding in the Callery River, Westland. *Doctoral dissertation*, Lincoln University.
- R, Nandhini. (2021). Tatar Stream Landslide Dambreak Flood Hazard Analysis. *Master's Dissertation*. University of Canterbury.

Robinson, T.R., Davies, T.R.H., Wilson, T.M. and Orchiston, C., 2016. Coseismic landsliding estimates for an Alpine Fault earthquake and the consequences for erosion of the Southern Alps, New Zealand. *Geomorphology*, 263, pp.71-86.

Welsh, A.J. and Davies, T.R.H., 2011. Identification of alluvial fans susceptible to debris-flow hazards. *Landslides*, 8(2), pp.183-194.

DRAFT